Small-angle neutron scattering study of structure and kinetics of temperature-induced protein gelation

S. Chodankar,[1] V. K. Aswal,[1] J. Kohlbrecher,[2] R. Vavrin,[2] and A. G. Wagh[1]
[1]*Solid State Physics Division, Bhabha Atomic Research Centre, Mumbai-400 085, India*
[2]*Laboratory for Neutron Scattering, ETH Zurich & Paul Scherrer Institut, CH-5232 Villigen PSI, Switzerland*
(Received 11 November 2008; published 11 February 2009)

The phase diagram, structural evolution, and kinetics of temperature-induced protein gelation of protein Bovine Serum Albumin (BSA) have been studied as a function of solution *p*H and protein concentration. The protein gelation temperature represents the onset of turbidity in the protein solution, which increases significantly with increasing *p*H beyond the isoelectric *p*H of the protein molecule. On the other hand, the gelation temperature decreases with an increase in protein concentration only in the low-protein-concentration regime and shows a small increasing trend at higher protein concentrations. The structural evolution and kinetics of protein gelation have been studied using small-angle neutron scattering. The structure of the protein molecule remains stable up to temperatures very close to the gelation temperature. On increasing the temperature above the gelation temperature, the protein solution exhibits a fractal structure, an indication of gel formation due to aggregation. The fractal dimension of the gel increases with increasing temperature, suggesting an increase in branching between the aggregates, which leads to stronger gels. The increase in both solution *p*H and protein concentration is found to delay the growth in the fractal structure and its saturation. The kinetics of gelation has been studied using the temperature-jump process of heating. It is found that the structure of the protein gels remains invariant after the heating time (~1 min), indicating a rapid formation of gel structure within this time. The protein gels prepared through gradual and temperature-jump heating routes do not always show the same structure. In particular, at higher temperatures (e.g., 85 °C), while gradual heating shows a fractal structure, there is collapse of such fractal structure during temperature-jump heating.

DOI: 10.1103/PhysRevE.79.021912 PACS number(s): 87.14.E−, 61.05.fg, 82.70.Gg

I. INTRODUCTION

The heating of a globular protein solution provokes conformational changes of the protein molecule, resulting in exposure of hydrophobic groups to the solvent. This triggers the aggregation of denaturated protein molecules, which eventually either precipitate or form a gel depending on the solution conditions [1–3]. The structure and properties of such gels depend on the strength of the interaction, predominantly on the intricate balance of attractive and repulsive forces between the protein molecules. The repulsive forces are considered to be induced by the surface charge, and the attractive forces are believed to originate from the hydrophobic residues exposed by the thermal denaturation of the protein [4–8]. The balance between these two opposing interactions depends on the *p*H that controls the net charge of the protein, the ionic strength of the solvent favoring the screening of the electrostatic interactions and the number of exposed hydrophobic groups deciding the amount of attraction among the molecules. It is found that protein solutions at a *p*H away from the isoelectric point and at low ionic strength form a fibril network translucent in appearance [9–11]. On the other hand, at a *p*H close to the isoelectric point and high ionic strength, densely cross-linked gels are formed [12–14]. The differences in these structures have been evidenced mainly by electron microscopy [15–17]. The gelation phenomenon of globular proteins has generated a great deal of challenge from both points of view of practical necessity and scientific interest. The properties of protein gels usually differ very much from those of physical gels of chainlike macromolecules such as polymers [18–21]. Protein gels possess many important practical properties such as low elasticity and high water-holding capacity. Furthermore, due to their immense health and texture related importance, they are used in a variety of food- and drug-related products.

The level of disruption of the protein structure and thus its reactivity to the neighboring protein molecule depend on the absolute value of the temperature and the mode of heating [22–25]. The temperature of heating is responsible for the different hydrophobic groups which can be exposed to the solvent and thus controls the rate at which aggregation or gelation takes place. On the other hand, the mode of heating (gradual or fast) is another important parameter that decides the route in which the gelation proceeds and thus defines the kinetics of the gelation. The mode of heating governs the rate of consumption of native proteins and their molecular approach for the growth or stagnation of gelation process [26–31]. These parameters together decide the structure and physical properties of the protein gels. Numerous studies have shown that protein aggregation leading to a network structure of protein gels results in the formation of fractal aggregates closely packed throughout the system [19,24–26]. The formation of the fractal aggregates and the corresponding fractal dimension represent the strength of the gels, whereas the saturation in the fractal structure indicates the completion of the gelation process. Small-angle neutron scattering (SANS) can be used for investigating the structure of such fractal aggregates in detail over a wide length scale [19]. However, there are only limited SANS studies [25,32,33] carried out at few temperatures, and further, no attempts have been made to study the kinetics.

In this paper, we report a SANS study of the structural evolution of temperature-induced protein gels over a wide

range of temperature (30–90 °C). The effect of solution *p*H and concentration on protein gelation has been examined. The kinetics of the gelation process is studied through temperature-jump measurements within a time interval of 1 min. The results of the temperature-jump measurements are also compared with the gradual heating mode of gelation.

II. EXPERIMENT

Bovine Serum Albumin (BSA) protein (catalog No. 05480) was purchased from Fluka. Samples for SANS experiments were prepared by dissolving a weighted amount of BSA in a buffer solution of D_2O. The use of D_2O as solvent instead of H_2O provides better contrast for hydrogenous protein in neutron experiments. Sample *p*H was adjusted at 5.5 using acetate buffer solution. The ionic strength of the solution was kept at 0.5 M NaCl to minimize the interparticle interaction among macromolecules. Small-angle neutron scattering experiments were performed on the SANS-I instrument at Swiss Spallation Neutron Source, SINQ, Paul Scherrer Institut, Switzerland [34]. The mean wavelength of the incident neutron beam was 8 Å with a wavelength resolution of approximately 10%. The scattered neutrons were detected using a two-dimensional 96×96 cm^2 detector. The experiments were performed at two sample-to-detector distances of 2 and 6 m, respectively, to cover the data in the wave-vector-transfer Q range of 0.006–0.25 Å^{-1}. The measured SANS data were corrected and normalized to a cross-sectional unit using BERSANS-PC data-processing software [35]. The effect of temperature on protein gelation has been observed up to 90 °C for all samples. The samples were heated gradually (~1 °C/min) and were provided an additional half an hour time in order for the gelation kinetics reach equilibrium. The *p*H dependence on protein gelation was compared at 1 wt % protein concentration for *p*H 6.5 with 5.5. The higher *p*H (6.5) was obtained using a phosphate buffer solution. The influence of the concentration on controlling the protein gelation was examined by comparing the results of 1 wt % with 5 wt % at *p*H 5.5. The temperature-jump experiment was performed on the protein samples by increasing the temperature to the required value within a time of about 1 min. This was achieved by immersing the sample of volume 1 ml in a water bath of large volume of 1000 ml maintained at a temperature of 5 °C higher than that of required temperatures. The SANS measurements were than performed on the sample at constant required temperature. Thereafter time-dependent SANS measurements were performed at every 1-min interval up to half an hour.

III. SMALL-ANGLE NEUTRON SCATTERING ANALYSIS

In small-angle neutron scattering one measures the coherent differential scattering cross section per unit volume $(d\Sigma/d\Omega)$ as a function of Q. For a system of monodispersed interacting protein macromolecules, $d\Sigma/d\Omega$ (Q) is expressed as [36]

$$\frac{d\Sigma}{d\Omega}(Q) = N_p V_p^2(\rho_p - \rho_m)^2[\langle F(Q)^2\rangle + \langle F(Q)\rangle^2(S_p(Q)-1)] + B, \tag{1}$$

where N_p and V_p are the number and volume of the protein macromolecule, respectively. ρ_p and ρ_m are the scattering length densities of the protein and solvent, respectively. $F(Q)$ is the single-particle form factor, and $S_p(Q)$ is the interparticle structure factor. B is a constant term that represents the incoherent scattering background, which is mainly due to hydrogen in the sample. In the case of protein solution at low concentration and at high salt concentration, $S(Q)$ can be approximated to unity as the interparticle interactions are minimized [37]. $F(Q)$ has been calculated for the prolate ellipsoidal shape of the protein macromolecules [38].

In the case of temperature-induced denaturation of proteins, it is believed that aggregation of protein molecules leads to gelation. For such a system the structure factor is not any longer negligible and has to be included in the description of the scattering cross section. The aggregation process starts with individual protein macromolecules, which aggregate into a larger network formation. The cross section for such a system can be expressed as [39]

$$\frac{d\Sigma}{d\Omega}(Q) \sim P_p(Q)S_f(Q) + B. \tag{2}$$

$P_p(Q)$ denotes the normalized intraparticle structure factor of a protein macromolecule in the cluster, which is the building block of the complex gel and can be considered to be an equivalent sphere of radius R_p. $P_p(Q)$ for a spherical particle of radius R_p is given by

$$P_p(Q) = \left[\frac{3(\sin QR_p - QR_p\cos QR_p)}{(QR_p)^3}\right]^2. \tag{3}$$

$S_f(Q)$ has been calculated using the fractal structure of the aggregated network. In this case, $S_f(Q)$ is given as [40,41]

$$S_f(Q) = 1 + \frac{1}{(QR_p)^D}\frac{D\Gamma(D-1)}{[1+(Q\xi)^{-2}]^{[(D-1)/2]}} \times \sin[(D-1)\tan^{-1}(Q\xi)], \tag{4}$$

where D is the fractal dimension of the gel and ξ is the correlation length that is a measure of the extent of the aggregated network. Throughout the data analysis, corrections were made for instrumental smearing. The parameters in the analysis were optimized by means of nonlinear least-squares fitting, and the errors (standard deviations) in the parameters were calculated by the standard method [42].

IV. RESULTS AND DISCUSSION

Figure 1 shows the phase diagram of the protein gelation temperature measured at various *p*H and protein concentration values. The data points in the phase diagram represent the temperature at which the protein solution turns into a gel, which is recorded visually by the appearance of turbidity and increase in viscosity of the solution. The effect of *p*H is carried out on 1 wt % protein solution in the *p*H range of

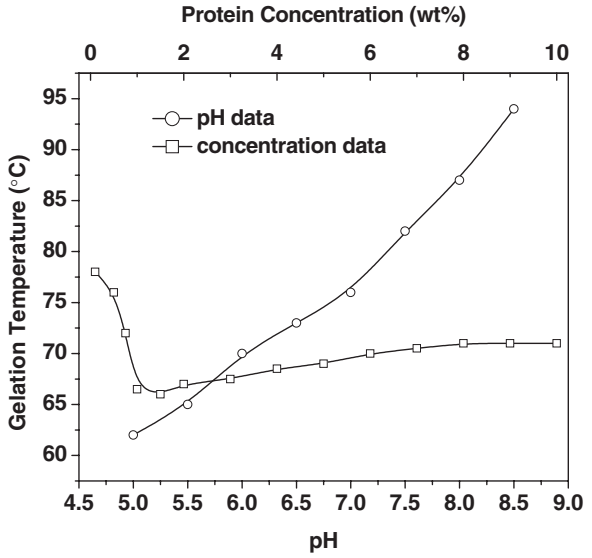

FIG. 1. Phase diagram of temperature-induced protein gelation with varying *p*H for 1 wt % BSA and varying protein concentration at fixed *p*H 5.5. The lines connecting the data points are a guide to the eye.

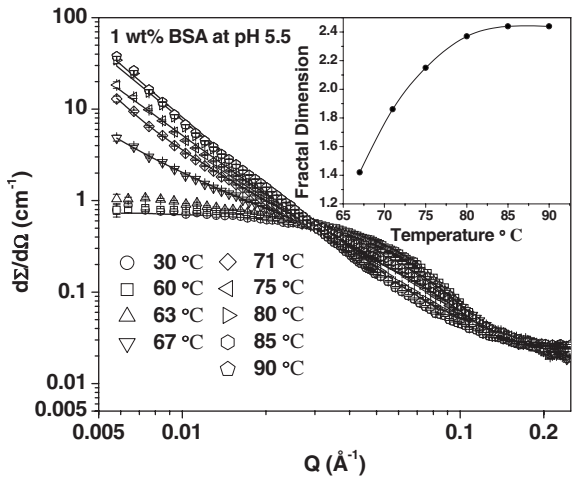

FIG. 2. Fitted SANS data for 1 wt % BSA at *p*H 5.5 as a function of temperature. The inset shows the temperature dependence variation of the fractal dimension of the gel, where the lines connecting the data points are only a guide to the eye.

5–8.5. The gelation temperature is found to be significantly affected by the change in *p*H of the solution, and it increases with an increase in the *p*H, having values above the isoelectric point of BSA protein (4.7). For example, at *p*H 5 the gelation occurs at a temperature of 62 °C, whereas the gelation temperature is increased to 94 °C at *p*H 8.5. This increase in gelation temperature with *p*H can be understood on the basis of the *p*H dependence electrostatic interaction between charged protein macromolecules. The protein molecule has nonzero net charge for *p*H values different from the isoelectric point, the magnitude of which increases as *p*H is varied away from the isoelectric point. Therefore, the gelation at higher *p*H values requires higher temperature to generate enough hydrophobic attraction that can overcome the increase of charge repulsion between them. A similar increase in gelation temperature with change in *p*H has also been observed for whey protein [43]. The role of varying concentration on the protein gelation temperature is carried out at several concentrations in the range 0.1–10 wt % for fixed *p*H 5.5 of the solution. The increase in protein concentration leads to an initial drop in gelation temperature, which increases marginally with further increase in protein concentration. The decrease in gelation temperature in the low-concentration regime is understood in terms of the solubility of the system decreases with increase in concentration. The slow increase in gelation temperature at higher concentrations could be due to marginal dominance of increased repulsive interactions between the molecules with that of the decrease in the solubility of the molecules. It may be mentioned that most of the studies in the literature on protein gelation have been carried out in H_2O [3,4,6]. Comparison of our data of protein gelation in D_2O with these earlier studies show that the gelation temperature is about 4–5 °C lower in D_2O with respect to H_2O. This is expected due to the lower solubility of protein in the case of D_2O.

To study structural evolution in protein solution during the process of gelation, Fig. 2 shows the SANS data for gelation of 1 wt % BSA at *p*H 5.5 as a function of temperature. The temperature of the protein sample is achieved by gradually heating the sample to the required temperature and giving enough time (half an hour) for heating at this temperature for the kinetics to reach equilibrium. The SANS data from room temperature up to 60 °C do not show any significant change in the scattering profile, suggesting that there is no prominent effect on the structure of the protein molecule, which thus maintains its native structure within this temperature range. This result is in agreement with a previous study using Fourier-transform infrared spectroscopy on temperature-induced denaturation [44], which showed no loss of the native structure up to a temperature of around 60 °C. At room temperature, the protein molecule fits to a monomeric model and is found to have a prolate ellipsoidal shape with semimajor and semiminor axes $a=70.2\pm5.1$ and $b=c=22.2\pm0.8$ Å, respectively, which are in good agreement with values reported earlier [45–47]. Data are also fitted for a system consisting of higher-mers [37], which further confirms that the protein solution mostly consists of monomers. On increasing the temperature beyond 60 °C, there is a buildup of scattering cross section in the low-Q region, which is an indication of the aggregation of protein molecules at higher temperatures. The increase in scattering

TABLE I. Fitted parameters of SANS analysis for gel structure of 1 wt % BSA at *p*H 5.5 as a function of temperature.

Temperature (°C)	Fractal dimension D	Protein radius R_p (Å)	Pore radius R_{pore} (Å)
67	1.42 ± 0.03	26.9 ± 1.3	
71	1.86 ± 0.04	26.0 ± 1.2	
75	2.15 ± 0.05	25.8 ± 1.2	
80	2.37 ± 0.07		6.6 ± 0.3
85	2.44 ± 0.08		6.0 ± 0.3
90	2.44 ± 0.08		6.1 ± 0.3

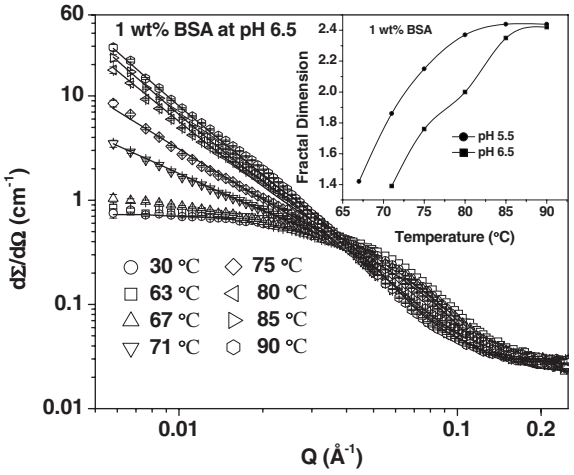

FIG. 3. Fitted SANS data for 1 wt % BSA at *p*H 6.5 as a function of temperature. The inset shows the comparison of the fractal dimension of gels for *p*H 6.5 with 5.5, where the lines connecting the data points are only a guide to the eye.

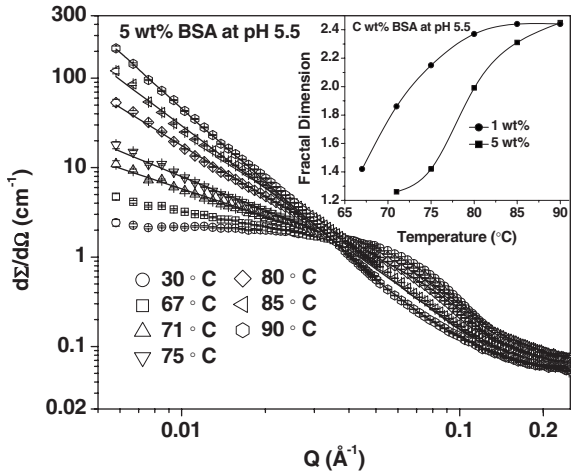

FIG. 4. Fitted SANS data for 5 wt % BSA at *p*H 5.5 as a function of temperature. The inset shows the comparison of the fractal dimension of gels for protein concentration 5 wt % with 1 wt %, where the lines connecting the data points are only a guide to the eye.

cross section suggests that the aggregation is enhanced with increasing temperature, which leads to gelation. The present system has a gelation temperature of 65 °C, and the SANS data beyond this temperature show a linear region of scattering cross section on a log-log scale for low values of $Q < 0.07$ Å^{-1}. This represents the fractal structure of a gel, which consists of a network kind of arrangement of protein aggregates in the system. The slope of the scattering data gives the value of the fractal dimension D of the network. The cutoffs of the linear range of the data at low and high Q values are, respectively, related to the extent of the aggregated network and the size of the building block of the network. The low-Q cutoff is not observed in Fig. 2, where the lowest Q value is $Q_{\min}=0.006$ Å^{-1}. This means that the aggregated network has a size ξ larger than $2\pi/Q_{\min}$ (i.e., 900 Å). Therefore, we have used a fixed value of 1000 Å for fitting of all data. The fitted parameters using Eq. (2) are given in Table I. It is found that the fractal dimension increases with increasing temperature. This is understood to be due to the increase in branching between the aggregated protein molecules with increasing temperature. The inset of Fig. 2 shows the variation of fractal dimension of the protein gelation at different temperatures. It is found that the fractal dimension of the system increases significantly with an increase in temperature and saturates at higher temperatures. The size of the building block of the aggregated network ($R_p \sim 27 \pm 1$ Å) has been found to be significantly smaller than the equivalent spherical radius $[(ab^2)^{1/3}=32.5 \pm 3.5$ Å] of the native structure of the protein. This can be possible due to protein undergoing different conformational changes while aggregation occurs [2,41]. The scattering cross section in the high-Q region at higher temperatures ($\geqslant 80$ °C) decreases significantly as well as there is a change in the functionality of the scattering profile. This kind of behavior is expected if the building blocks of the fractal structure are not visible any longer to neutrons and what is seen are the pores between the building blocks as a result of increased packing of the building blocks at higher temperatures. The typical radius of the pore structure obtained in protein gels is about 6 Å.

The effect of *p*H on the temperature-induced protein gelation is shown in Fig. 3 for *p*H 6.5 and compared to the data of *p*H 5.5 (Fig. 2). The general features of the scattering profiles for the two *p*H values on varying temperature are similar. However, the temperature required to generate similar results is considerably higher for the protein samples at *p*H of 6.5 than 5.5. This can be correlated to the increase in the gelation temperature for higher *p*H values where the gelation process is delayed as a function of temperature. The inset of the Fig. 3 shows the comparison of the variation of

TABLE II. Fitted parameters of SANS analysis for gel structure of 1 wt % BSA at *p*H 6.5 as a function of temperature.

Temperature (°C)	Fractal dimension D	Protein radius R_p (Å)	Pore radius R_{pore} (Å)
71	1.38 ± 0.03	26.5 ± 1.3	
75	1.76 ± 0.04	26.4 ± 1.3	
80	2.00 ± 0.07	26.3 ± 1.3	
85	2.35 ± 0.08		5.9 ± 0.3
90	2.42 ± 0.07		5.5 ± 0.2

TABLE III. Fitted parameters of SANS analysis for gel structure of 5 wt % BSA at *p*H 5.5 as a function of temperature.

Temperature (°C)	Fractal dimension D	Protein radius R_p (Å)	Pore radius R_{pore} (Å)
71	1.21 ± 0.03	26.3 ± 1.3	
75	1.42 ± 0.03	25.9 ± 1.2	
80	1.99 ± 0.05	26.4 ± 1.3	
85	2.31 ± 0.07		5.9 ± 0.3
90	2.45 ± 0.11		5.5 ± 0.2

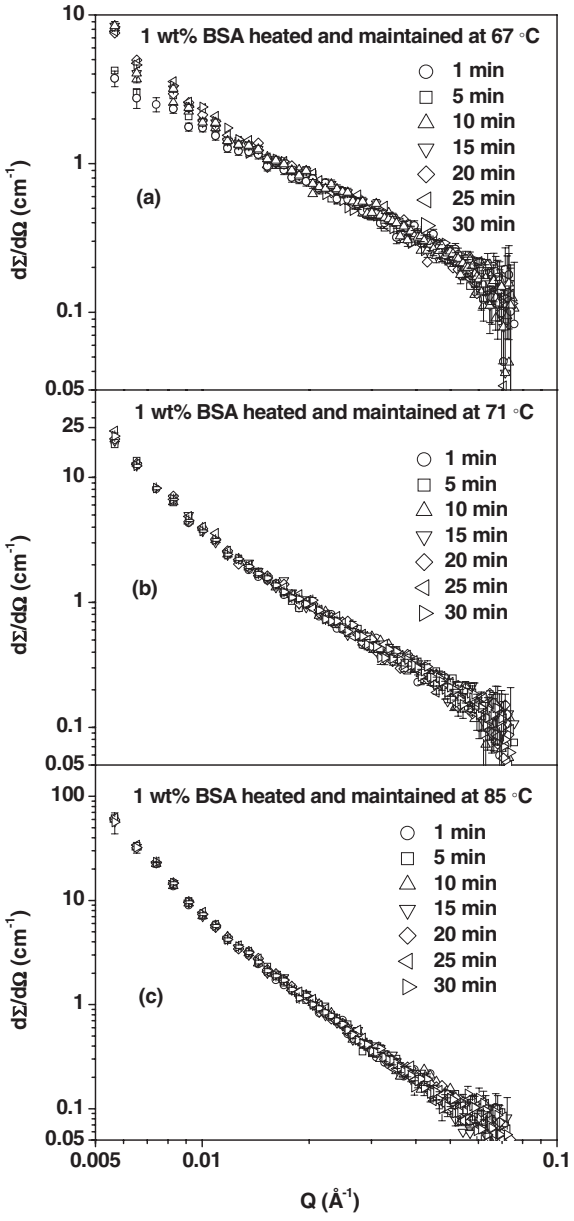

FIG. 5. Time-resolved SANS data for 1 wt % BSA at *p*H 5.5 heated through the temperature-jump process at temperatures (a) 67 °C, (b) 71 °C, and (c) 85 °C.

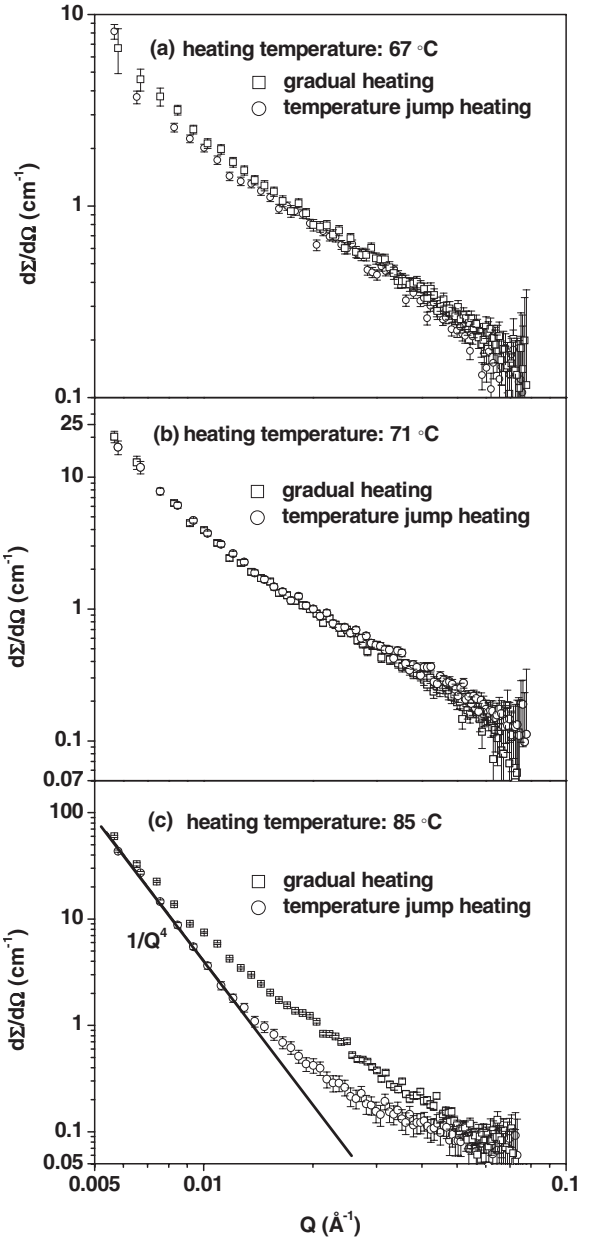

FIG. 6. Comparisons of equilibrated SANS data of 1 wt % BSA at *p*H 5.5 as obtained by temperature jump and gradual heating at (a) 67 °C, (b) 71 °C, and (c) 85 °C.

fractal dimension with rise in temperature for *p*H 6.5 with 5.5. It can be seen that the temperature dependence growth of fractal structure is quite different for two *p*H values. Both the formation of fractal structure and saturation occurs at higher temperature for higher *p*H value. The fitted parameters of the temperature-induced protein gels at *p*H 6.5 using Eq. (2) are given in Table II.

To understand the role of concentration, SANS data were collected for 5 wt % BSA at *p*H 5.5 (Fig. 4) to compare with the data of 1 wt % BSA at *p*H 5.5 (Fig. 2). It is found that on increasing the protein concentration there is about a 5 times increase in scattering intensity in the overall Q range with respect to Fig. 2. However, the scattering cross-section profiles have similar features to Fig. 2. On the other hand, the temperature required to get similar gel structures is significantly higher for protein gels at higher protein concentration similar to that of increasing *p*H value (Fig. 3). The inset of Fig. 4 shows the comparison of the variation of fractal dimension with rise in temperature for 1 and 5 wt % BSA protein gels. It is observed that growth of fractal structure significantly depends on the protein concentration. At higher concentration the formation of fractal structure is delayed and the saturation in the structure is not observed even up to 90 °C. The fitted parameters of the temperature-induced protein gels at 5 wt % using Eq. (2) are given in Table III.

The kinetics of protein gelation has been studied through temperature-jump experiments. The temperature-jump process is carried out by increasing the temperature of the sample instantaneously (~1 min) to the required tempera-

ture and maintaining it during the measurements. The time-resolved measurements are then performed to measure kinetics of these samples. Figure 5 shows the time-resolved SANS data in the limited Q range for 1 wt % BSA at three different temperatures. The three different temperatures selected for these studies correspond to different protein gel structures. The SANS data were recorded at every 1 min up to 30 min; however, only limited data are shown in Fig. 5. It is found that the data do not show any significant change as time progresses. This suggests that the kinetics of structural evolutions that lead to gelation occurs fast within the time of temperature jump ($\sim$1 min). It can be added that the data of protein gel at 67 °C show some changes as compared to that at higher temperature. This could be due to the fact that at temperature near the gelation temperature the gel has somewhat slower kinetics than at higher temperatures.

Figure 6 shows the comparison of SANS data of the protein gels as prepared by temperature jump with that by gradual heating. It is seen that the structure of the gels prepared at lower temperatures (67 and 71 °C) remains similar irrespective of the mode of heating. However, when the temperature is increased to 85 °C, the results of the two heating modes are significantly different. It can be understood in terms of the fact that at temperatures not far from the gelation temperature, the process of gelation is site specific for both modes of heating. As the temperature is gradually increased, the site-specific process of gelation is continued. On the other hand, in temperature-jump heating at higher temperatures the branching of the protein aggregates collapses because the site specificity of aggregation does not work anymore by the sudden rise of temperature. This point is verified by the fact that the gel structure formed at 85 °C by temperature-jump heating shows a slope of −4 on a log-log scale, an indication of the collapsed large aggregates, which is very different than the fractal structure of gel obtained by gradual heating (Table I).

V. CONCLUSIONS

The effect of *p*H and protein concentration on temperature-induced protein gelation has been studied using phase diagrams and SANS. The gelation temperature of the protein is found to increase considerably with increasing *p*H beyond isoelectric *p*H of the protein molecule. However, the increase in protein concentration leads to a decrease in gelation temperature in the low-protein-concentration regime and shows a small increasing trend at higher protein concentrations. The protein gel is characterized by a fractal structure whose fractal dimension increases due to enhanced branching of the aggregates with increase in temperature. The increase in both solution *p*H and protein concentration delays the growth of the temperature-dependent fractal structure and its saturation. The temperature-jump study of the kinetics of protein gels suggests a rapid formation of gel structure within a time of 1 min. It is also found that the structure of protein gel in particular prepared at high temperatures depends on the route of heating (gradual or temperature jump).

ACKNOWLEDGMENT

This work is based on SANS experiments performed at the Swiss spallation neutronsource SINQ, Paul Scherrer Institut, Villigen, Switzerland.

[1] C. R. Cantor and P. R. Schimmel, *Biophysical Chemistry* (Freeman, San Francisco, 1980).
[2] W. S. Gosal and S. B. Ross-Murphy, Curr. Opin. Colloid Interface Sci. **5**, 188 (2000).
[3] W. G. Griffin, M. C. A. Griffin, S. R. Martin, and J. Price, J. Chem. Soc., Faraday Trans. **89**, 3395 (1993).
[4] J. Gimel, D. Durand, and T. Nicolai, Macromolecules **27**, 583 (1994).
[5] F. Meersman and K. Heremans, Biochemistry **42**, 14234 (2003).
[6] X. L. Qi, C. Holt, D. Mcnulty, D. T. Clarke, S. Brownolow, and G. R. Jones, Biochem. J. **324**, 341 (1997).
[7] C. Tanford, K. Kawahara, and S. Lapanje, J. Am. Chem. Soc. **89**, 729 (1967).
[8] T. Matsumoto and H. Inoue, J. Chem. Soc., Faraday Trans. **87**, 3385 (1991).
[9] A. H. Clark, *Functional Properties of Food Macromolecules* (Aspen, London, 1998).
[10] M. M. Ould Eleya, S. Ko, and S. Gunasekaran, Food Hydrocolloids **18**, 315 (2004).
[11] M. Reif, M. Gautel, F. Oesterhelt, J. M. Fernandez, and H. E. Gaub, Science **276**, 1109 (1997).
[12] M. Pouzot, T. Nicolai, D. Durand, and L. Benyahia, Macromolecules **37**, 614 (2004).
[13] M. Pouzot, L. Benyahia, and T. Nicolai, J. Rheol. **48**, 1123 (2004).
[14] G. M. Hall, *Methods of Testing Protein Functionality* (Blackie Academic and Professional, New York, 1996).
[15] K. Nishinari, H. Zhang, and S. Ikeda, Curr. Opin. Colloid Interface Sci. **5**, 195 (2000).
[16] N. S. Hettiarachchy and G. R. Ziegler, *Protein Functionality in Food Systems* (CRC Press, Boca Raton, 1994).
[17] L. G. B. Bremer, T. van Vliet, and P. Walstra, J. Chem. Soc., Faraday Trans. 1 **85**, 3359 (1989).
[18] A. Tobitani and S. B. Ross-Murphy, Macromolecules **30**, 4845 (1997).
[19] A. H. Clark, G. M. Kavanagh, and S. B. Ross-Murphy, Food Hydrocolloids **15**, 383 (2001).
[20] K. Yasuda, R. Nakamura, and S. Hayakawa, J. Food. Sci. **51**, 1289 (1986).
[21] R. S. Meyer, K. L. Cooper, D. Knorr, and H. L. M. Lelieveld, J. Food Technol. **54**, 67 (2000).
[22] S. Ikeda and K. Nishinari, Biopolymers **59**, 87 (2001).
[23] E. H. C. Bromley, M. R. H. Krebs, and A. M. Donald, Eur. Phys. J. E **21**, 145 (2006).
[24] M. Langton and A. M. Hermansson, Food Hydrocolloids **10**, 179 (1996).
[25] W. S. Gosal, A. H. Clark, and S. B. Ross-Murphy, Biomacro-

molecules **5**, 2408 (2004).
[26] S. B. Ross-Murphy, Phys. Chem. Chem. Phys. **102**, 1534 (1998).
[27] M. Pouzot, T. Nicolai, W. V. Visschers, and M. Weijers, Food Hydrocolloids **19**, 231 (2005).
[28] G. Panik, R. Malessa, R. Winter, G. Rapp, K. J. Frye, and C. A. Royer, J. Mol. Biol. **275**, 389 (1998).
[29] S. Ikeda, E. A. Foegeding, and T. Hagiwara, Langmuir **15**, 8584 (1999).
[30] M. Verheul, S. P. F. M. Roefs, J. Mellema, and K. G. de Kruif, Langmuir **14**, 2263 (1998).
[31] M. Stading and A. M. Hermansson, Carbohydr. Polym. **22**, 49 (1993).
[32] C. C. Chang, Y. C. Su, M. S. Cheng, and L. S. Kan, Phys. Rev. E **66**, 021903 (2002).
[33] P. Aymard, T. Nicolai, and D. Durand, Macromolecules **32**, 2542 (1999).
[34] J. Kohlbrecher and W. Wagner, J. Appl. Crystallogr. **33**, 804 (2000).
[35] U. Keiderling, Appl. Phys. A: Mater. Sci. Process. **74**, S1455 (2002).
[36] J. B. Hayter and J. Penfold, Colloid Polym. Sci. **261**, 1022 (1983).
[37] S. Chodankar and V. K. Aswal, Phys. Rev. E **72**, 041931 (2005).
[38] J. S. Pedersen, Adv. Colloid Interface Sci. **70**, 171 (1997).
[39] P. W. Schmidt, J. Appl. Crystallogr. **24**, 414 (1991).
[40] J. Teixeira, J. Appl. Crystallogr. **21**, 781 (1988).
[41] S. Chodankar, V. K. Aswal, J. Kohlbrecher, R. Vavrin, and A. G. Wagh, Phys. Rev. E **77**, 031901 (2008).
[42] P. R. Bevington, *Data Reduction and Error Analysis for Physical Sciences* (McGraw-Hill, New York, 1969).
[43] Z. U. Haque and M. Sharma, J. Agric. Food Chem. **45**, 2958 (1997).
[44] K. Murayama and M. Timoda, Biochemistry **43**, 11526 (2004).
[45] S. Chodankar, V. K. Aswal, J. Kohlbrecher, R. Vavrin, and A. G. Wagh, J. Phys.: Condens. Matter **19**, 326102 (2007).
[46] E. Seth and V. K. Aswal, J. Macromol. Sci., Phys. **B42**, 85 (2003).
[47] S. H. Chen and J. Teixeira, Phys. Rev. Lett. **57**, 2583 (1986).